Establishment of a ground surface temperature map for climate change response on the basis of Landsat 8 OLI satellite images

Vu Thi Thu Hien[1], *Tran Thanh* Son[1*], *Duong Thi Mai* Chinh[1], and *Le Thi Hoa* Hue[1]

[1]Branch of Hanoi University of Natural Resources and Environment in Thanh Hoa province, Vietnam

Abstract. In recent years, in Vietnam, there have been studies using the thermal infrared channel to estimate the surface temperature value, studies using Plank's formula to estimate the surface temperature value from the thermal infrared channel without using the surface emissivity, using the emissivity as a common constant for coating objects [1 – 4]. In the area of Bim Son town – Thanh Hoa province – Vietnam, along with the process of urbanization as well as socio-economic development, the quality of the urban environment, surface coverage by plants and use activities have been greatly affected, especially the limestone mining for cement of one of the largest cement plants in the country (Bim Son cement plant) has had a significant impact on the temperature of the area. The monitoring results have not provided an overview of the temperature background of the whole area of Bim Son town in the period of 2017-2023 in order to assess the change in the temperature background of the region, thereby providing solutions to respond to climate change. The article uses Landsat 8 OLI satellite images to establish a surface heat map for the assessment of climate change for the area of Bim Son – Thanh Hoa, thereby making more general assessments for other areas in Vietnam. The experimental results were compared and evaluated to show the relevance of the data as well as the image processing process.

1 Introduction

Over the years, with the trend of innovation and integration, Vietnam has created new impulses for the development process, overcoming the impact of the global recession and maintaining the annual economic growth rate with an average of 5.7 %/year. However, in addition, we are facing many challenges, including the problem that the increase in surface temperature has been seriously affecting the quality of the living environment of people and organisms. The increase in surface temperature also affects meteorological factors such as humidity, rainfall...and increases the frequency of other natural disasters. The impact of urbanization on the thermal environment is to create an "Urban Heat Island" effect. The phenomenon occurs when at the same time, the temperature in the city, urban areas and industrial parks is greater than the temperature of neighboring or suburban areas. There are

* Corresponding author: ttson.ph@hunre.edu.vn

many factors that cause the formation of urban "heat islands", but the decline of vegetation cover is the first factor, the replacement of the soil surface with impermeable materials makes the amount of water entering the atmosphere less than the natural surface. Therefore, surface temperature is considered an important parameter that characterizes the energy exchange between the land surface and the atmosphere. Land surface temperature is considered an important variable in the study of drought, soil moisture, detection and monitoring of wildfires, underground fires in coal mines [5].

Current remote sensing technology allows detailed analysis of surface temperature changes over a large area without being limited by the number of measurement points such as meteorological stations. The meteorological stations only accurately reflect the local temperature around the measuring station, but not the whole area. Landsat satellite images obtained from Landsat TM sensors with a thermal channel resolution of 120 m, Landsat ETM + 60 m and Landsat 8 with TIRS (Thermal Infrared Sensor) sensors are used quite commonly in urban surface heat change research [2]. Currently, one of the common methods of calculating surface temperature is to convert numerical values (DN, Digital values) to Radiometric values directly from thermal infrared channels, thereby using algorithms to calculate surface temperature [2, 6]. In addition to the energy source from the sun reaching the earth's surface, the surface temperature is also affected by the surface emissivity and the effects of the atmosphere, so methods are needed to eliminate this diffraction. In addition, the surface emissivity also depends on the type of surface and ground cover.

2 Materials and methods

2.1 Surface temperature and the association with climate change

Land surface temperature (LST) is defined as the average radiated surface temperature of an area. It is the result of the synthesis of the interaction and exchange of energy between the atmosphere and the ground, and the balance between solar thermal radiation and atmospheric and ground flux on a regional and global scale. Surface temperature is an important indicator of the energy balance on the Earth's surface as well as of the greenhouse effect. This parameter determines the air temperature on the surface of the land and the long wave radiation between the ground and the atmosphere, as well as affects other phenomena on the ground, such as the amount of precipitation and surface radiation and reflections (Albedo).

Climate change is the change of the climate system including atmosphere, hydrosphere, biosphere, lithosphere, ice atmosphere now and in the future by natural and man-made causes in a certain period of decades or millions of years. The change can be an average change in the weather or a change in the distribution of weather events around an average. Climate change may be limited to a certain region or may occur throughout the Earth. In recent years, especially in the context of environmental policy, climate change often refers to current climate change, collectively referred to as global warming. The main cause of Earth's climate change is an increase in activities that generate greenhouse gas emissions, over-exploitation of absorption tanks and greenhouse gas reservoirs such as biomass, forests, other marine, coastal and inland ecosystems.

2.2 LandSat thermal infrared remote sensing images used as a database to establish heat maps

Landsat 8 (LDCM) carries two sensors: the Operational Land Imager (OLI) and the Thermal Infrared Sensor (TIRS). These sensors are designed to improve performance and reliability over previous generation Landsat sensors. These two sensors will provide seasonal surface detail at a spatial resolution of 30 meters (in the visible, near-infrared, and short-wave infrared channels); 100 meters in the heat channel and 15 meters in the full-color channel.

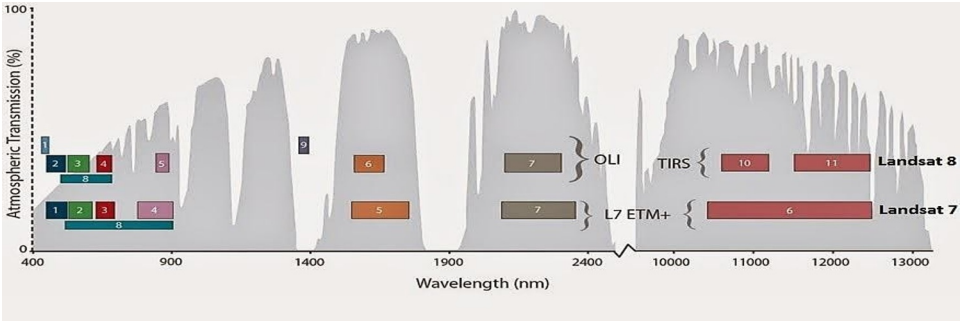

Fig. 1. Spectral channel characteristics of Landsat 7 ETM+ and Landsat 8 images [13].

2.3 Calculation of land surface temperature index from Landsat 8 OLI IMAGE

2.3.1 Convert numerical value (DN) to spectral radiation energy value (L_λ)

Landsat satellite image data after being collected will conduct radiation correction that converts numerical values to spectral reflected energy values and these correction formulas depend on the type of Landsat image. The calculation of the spectral reflection value for Landsat 8 is not related to the spectral radiation value, so it is possible to skip the step of calculating the spectral radiation value of each channel and switch to direct calculation according to the following formulas:

$$L_\lambda = M_L \times Q_{cal} + A_L \quad (1)$$

In which: L_λ is the spectral radiation value; ML: coefficient for each specific image channel (radius_MULT_BAND_x value in Landsat 8 image metadata file, where x is the image channel); for band 10 of Landsat 8 image, ML = 0.0003342; Qcal: numerical value of the image channel; AL: coefficient for each image channel (radius_ADD_BAND_x value in Landsat 8 image metadata file, where x is the image channel) for band 10 of Landsat 8 image, AL = 0.1. Seven, eight.

2.3.2 Calculate the luminous temperature value

Convert the radiation Toa (*Top of Atmosphere*) value to the luminance temperature Toa value using the formula (2) with the thermal constant provided in the Landsat image metadata file, for the Landsat 8 image band 10 K1 = 774.8853 ; K2 = 1321.0789 [1, 5, 9]

$$T_B = \frac{K_2}{\ln\left(\frac{K_1}{L} + 1\right)} - 273.15 \quad (2)$$

2.3.3 Calculation of emissivity

The emissivity of natural surfaces varies due to different ground cover characteristics, such as differences between fields, urban areas, and vacant land [1, 9-10]. Surface emissivity (ε) is calculated based on the formula (3) as follows: [1, 11]

$$\varepsilon = mP_v + n\ ; \quad m = \varepsilon_v - \varepsilon_s - (1 - \varepsilon_s)F\varepsilon_v\ ; n = \varepsilon_s(1 + \varepsilon_s)F\varepsilon_v \quad (3)$$

Where εv, εs are the surface emissivity of the vegetation-covered surface and vacant soil, respectively. The reference values for εv and$_{\varepsilon s}$ are 0.99 and 0.97, F is the shape index, assuming the geometric distribution is different and F = 0.55 [1, 12-13], respectively . Therefore, the formula (3) is specifically expressed by the formula (4) as follows:

$$\varepsilon = 0.004 * P_v + 0.986 \quad (4)$$

Where ε: emissivity; Pv: Proportion *of Vegetation*.
The plant component is calculated according to the formula:

$$P_v = \left(\frac{NDVI - NDVI_{min}}{NDVI_{max} - NDVI_{min}}\right)^2 \quad (5)$$

Where: Pv is the plant component value; NDVImin and NDVImax values are in the range of -1 to 1.

2.3.4 Calculate NDVI value

NDVI is a standard algorithm designed to estimate the quality of green vegetation on the ground by reflection measurement at red and near-infrared wavelengths. To calculate the NDVI value, apply the following formula:

$$NDVI = \left(\frac{NIR - Red}{NIR + Red}\right) \quad (6)$$

In which: NDVI is the plant index; NIR (*Near Infrared*) is the near-infrared channel of Landsat 8 remote sensing images; Red channel: The image channel belongs to the red visible light area of Landsat 8 images.

2.3.5 Estimated surface temperature

Land surface temperature LST (Ts) is the radiation temperature calculated using the luminosity temperature, the wavelength of the emitted radiation, the ground surface emissivity according to the formula (7) as follows [1, 3]:

$$T_S = \frac{T_B}{1 + \left(\lambda . \frac{T_B}{\rho}\right) . Ln(\varepsilon)} \quad (7)$$

$$\rho = \frac{h.c}{\sigma}\sigma = 1{,}438 \times 10^{-2}\, MK)\rho \times 10^{-23}$$

2.4 Technological process

Main steps of the process:

The study procedure was carried out as follows:

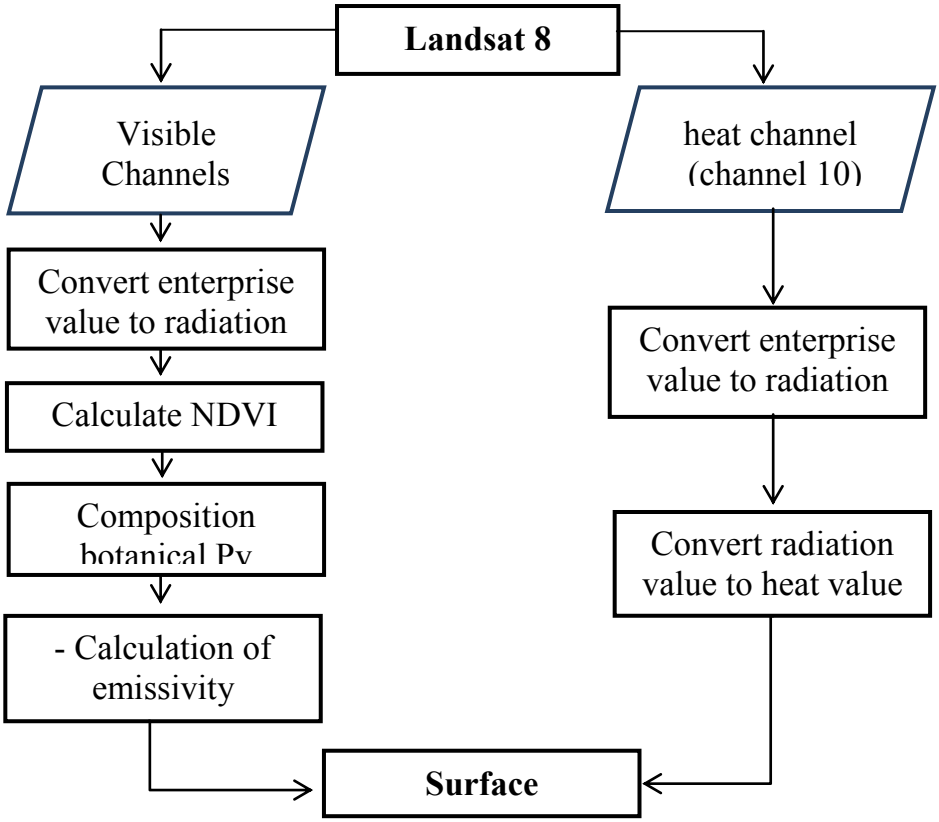

Fig. 2. Diagram of the process establishing a surface temperature map from Landsat 8 OLI.

3 Experimental results of surface temperature mapping from LandSat 8 OLI IMAGES

3.1 Experimental areas and databases

Landsat image data in Bim Son area was collected on July 31, 2017 and July 7, 2023 (*earthexplorer.usgs.gov*), daytime photos with good image quality and less impact by clouds (cloud ratio < 10%), coordinates UTM-WGS-84 zone 48 North (VN2000) according to Table 1.

Table 1. Landsat image data in Bim Son.

No.	Remove image	Recording date	Spatial Resolution
1	Landsat 8 images	31/07/2017	30
2	Landsat 8 images	07/07/2023	30

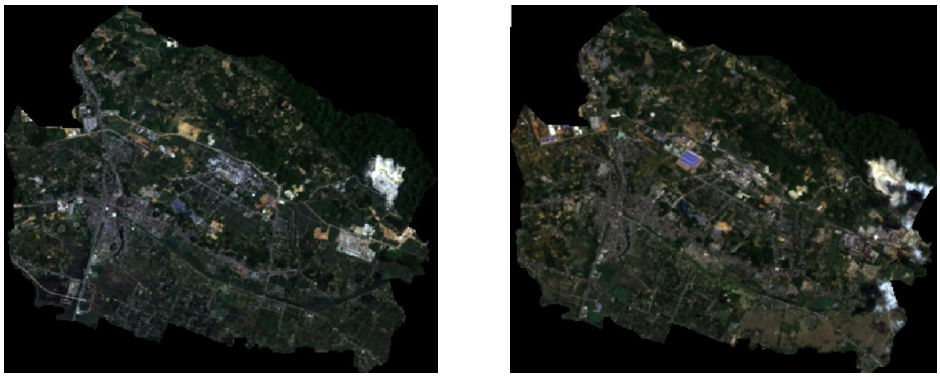

(a) ***(b)***

Fig. 3. Crop photo of the study area taken on July 31, 2017 (a) and photo taken on July 7, 2023 (b).

The surface temperature image of the LST in the study area follows the process (Figure 2), including the following main steps:

- Convert the numerical value to the radiation value: Use the Radiometric Calibration tool to convert the numerical value of the image to the thermal radiation value.
- *Calculate the NDVI plant index*: Use the *NDVI Calculation* tool to calculate the plant index for the image. As a result, we get NDVI images for 2 periods.
- Calculate Pv (the ratio of plants in a pixel): Use the Band Math tool to calculate the ratio of plants in a pixel according to the formula (5).
- *Calculate the index ε*: Use the Band Math tool to calculate the index according to the formula: $\varepsilon = 0.004\ Pv + 0.986$.
- *Calculate the transmittance of emission on the thermal infrared channel (channel 10,11).*

Surface temperature.

Using the Band Math tool, calculate the surface temperature for Landsat 8 images in Bim Son two periods (2017; 2023) according to the formula: b1-273.15

We have an image of the LST surface temperature of the study area.

The selection of 02 photos of the same month (07/2017; 07/2023) to facilitate the determination of temperature on an area that is not affected by conditions such as: season of the year; day and night.

Table 2. Statistics of the highest and lowest temperatures in Bim Son area.

No.	Year of shooting		Tmax(C0)
1	31/07/2017	24.7	34 * 2
2	07/07/2023	22.3	35.6

Through the temperature statistics from the two processed images, we see that the lowest temperature, the highest temperature of the area in 2017 is T_{min}= 24.70C; T_{max} =34.2^{o}C; 2023Tmin = 22.3^{o}C; T_{max}= 35.6^{o}C. Thus, we can see that within 6 years, the highest temperature value increases by 1.4^{o}C, an average of 0.230Cper year; the lowest temperature

decreases by 2.40C on average, adecrease of 0.40C per year, which proves that the markedly variable land surface temperature greatly affects global climate change.

To build a temperature map from the Tmin values, the T_{max} of the study area selects 6 levels to divide the temperature change interval ($T \leq 25C^0; 25C^0 \leq T \leq 27C^0; 27C^0 \leq T \leq 29C^0; 29C^0 \leq T \leq 31C^0; 31C^0 \leq T \leq 33C^0; T \geq 33C^0$.

We have the results of analysis of remote sensing images that have determined the area and distribution of surface temperature in Bim Son town on July 31, 2017, July 7, 2023 as follows:

We have the results of analysis of remote sensing images that have determined the area and distribution of surface temperature in Bim Son town on July 31, 2017, July 7, 2023 as follows:

Table 3. Area of heat levels in Bim Son town over the years.

No.	Temperature Threshold	Area (ha)		Area of difference
		31/07/2017	07/07/2023	
1	< 25	15.010	162.609	147.60
2	25 - 27.	3577.041	2926.951	650.09
3	27-29	2456.623	2531.807	75.18
4	29-31	258.765	654.431	395.67
5	(31~33)	6.810	31.049	24.24
6	Over 33	1.556	8.872	7-32

Surface temperature mapping was performed using Arcgis 10.4 software

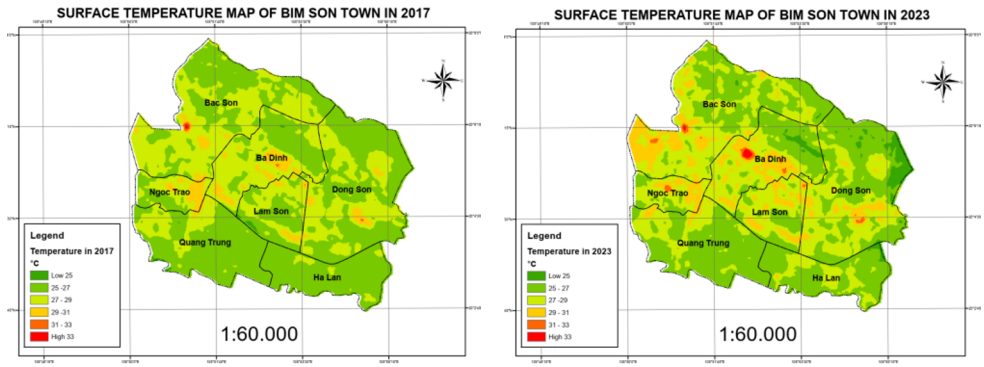

Fig. 4. Surface temperature map of Bim Son town area taken on July 31, 2017 and July 7, 2023.

The error in assessing the accuracy of the temperature determination method is determined from the mean Bias deviation and the error E (%) between the estimated values from satellite images and the actual measured values from the meteorological station according to the following formula [15]:

$$Bias = \frac{1}{N}\sum_{i=1}^{N}(T_{Si}^{tính} - T_{Si}^{đo}) \quad (8)$$

$$E(\%) = \frac{\left|T_{Si}^{tính} - T_{Si}^{đo}\right|}{T_{Si}^{đo}} \times 100 \quad (9)$$

In this paper, due to the limitation of measurement data, it is recommended to use the average temperature value at Bim Son town hydrometeorological station to calculate the error. The measurement temperature T(measured) 07/ 2017 is taken from the monthly

average temperature data corresponding to the month being photographed (July 2017) [14], 2023 is taken from the climate and weather data of the whole year in the area of Bim Son [16]; Calculated temperature is determined by the average value of Tmin and Tmax on the day being photographed. Assessment results are shown in the following table:

Table 4. Error in calculating the temperature over the time of shooting.

Time of capture		T (calculate)^{o}C	Deviation (Bias)	Measurement uncertainty
31/07/2017	29.9 (July 2017)	29.45	45	1.51
From 07/07/2023	28.1 (July 2023)	28.95	0.85	3.02

Previous studies have demonstrated that the error of temperature determination from satellite images ranges from 0.5-2^{o}C when there is adequate atmospheric correction and depending on different calculation methods. Therefore, the error value calculated in Table 4 is acceptable, the method of determining surface heat from the satellite is reliable, can be used to support environmental problems and climate change, in the condition that the ground measurement station grid is lacking.

3.2 Assessment of heat fluctuations in Bim Son town in the period of 2017-2023

From the two-period heat map, stacking, analyzing and evaluating surface temperature fluctuations based on the threshold heat levels, we established a map of land surface temperature fluctuations in the area of Bim Son town in the period 2017-2023.

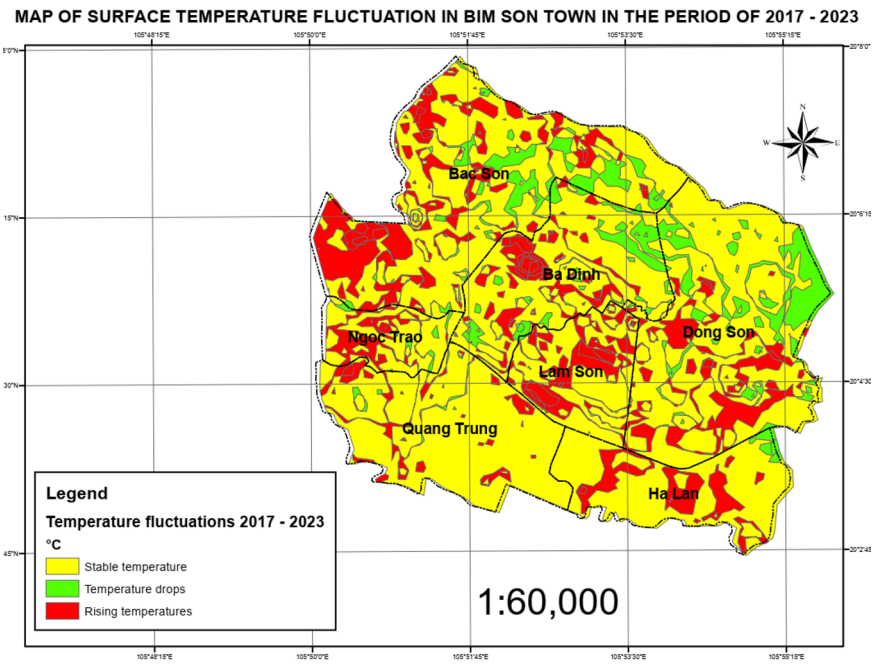

Fig. 5. Map of surface temperature fluctuations in Bim Son town in the period of 2017 - 2023.

After analyzing remote sensing images, it was determined the area and distribution of fluctuating surface temperatures in Bim Son town in the period of 2017 – 2023 as follows:

Table 5. Surface temperature fluctuation area in Bim Son town in the period of 2017 – 2023.

No.	Volatility Type	Variable area (ha)
1	Stability	4482.31
2	Temperature	562.82
3	Nhiet do tang	1270.68

From Table 5 shows that temperature fluctuations in Bim Son town in the period of 2017 – 2023 mainly remain stable (accounting for 71%), distributed relatively evenly in the whole town; areas with increased thermal background account for 20% are mainly distributed in densely populated urban areas such as Ba Dinh, Ngoc Trao, Lam Son wards due to the industrialization and urbanization taking place here; areas with relatively little decrease in temperature (accounting for 9%) are concentrated in communes outside of the town such as Dong Son, Bac Son wards...where mainly agricultural and non-agricultural land is located.

4 Conclusion

The paper developed a process using Landsat 8 OLI images to establish a surface temperature map of Bim Son town, Thanh Hoa province through the method of determining surface temperature by calculating the emission coefficient applying the NDVI plant index (for channel 4.5) and calculating the radiation coefficient for thermal channel 10. This method has the advantage of calculating the exact emission and radiation coefficient values on each pixel, so the level of detail and accuracy of the surface temperature maps of the study area is high (error from 1.51-3.02%).

Based on the establishment of two surface temperature maps and 01 temperature fluctuation map in Bim Son town in the period of 2017 - 2023, it can be seen that within 6 years (2017-2023), the highest temperature value (in the same month of July) of T_{max} increased by 1.4^{o}C, an average annual increase of 0.23^{o}C; the lowest temperatureof T_{min} decreased by 2.4^{o}C, an average annual decrease of 0.4^{o}C, which proves that the markedly variable land surface temperature greatly affects the climate change of the study area in particular and the global climate in general.

The results received in the study are also an important source of information to help managers take appropriate measures in sustainable urban development planning, minimize the impact of surface temperature fluctuations on the environment, thereby providing response plans to climate change for each region and certain stages.

References

1. N.T. Can, N.T.H. Diep, I. Sanwit, V. Pariwate, V.Q. Minh, Analysis of factors affecting the surface urban heat island phenomenon in Bangkok urban area, Thailand., Scientific Journal of Vietnam National University, Hanoi, Journal of Earth and Environmental Sciences (2019)
2. Le Van Anh, Tran Tuan Anh, "Study of soil surface temperature using the method of calculating emissivity from plant index," Journal of Earth Sciences, **36**, **2**, 184-192 (2014)
3. Tran Thi An, Nguyen Thi Dieu, Truong Phuoc Minh, Study of land surface temperature in Da Nang city from Landsat 7 ETM+ satellite image data, National GIS Application Workshop (2011)

4. Tan Thi Van, Hoang Thai, Le Van Trung, Thermal remote sensing method in urban surface temperature distribution research, Journal of Earth Sciences, 31 (2009)
5. Tran Thi Van, Hoang Thai, Le Van Trung, "Study of urban surface temperature change under the impact of urbanization in Ho Chi Minh City by remote sensing method," Journal of Earth Science, **33**, **3**, 347-359 (2011)
6. J.A. Sobrino, J.C. Jimenez-Munoz, L. Paolini, "Land suface temperature retrieval from LANDSAT TM5," Remote Sensing of Environment, **90**, **4**, 434-440 (2004)
7. L.D. User's, Department of the Interior U.S. Geological Survey. Handbook, USA (2016)
8. L.C. t. Radiance, Reflectance and At–Satellite Brightness Temperature, NASA
9. T.L. Hung, Application of Landsat thermal infrared imaging in the study of underground fire in coal mines, Journal of Pedagogical University of Ho Chi Minh City (2014)
10. Tran Thanh Son, Geodetic monitoring of high-rise structures according to satellite determinations, E3S Web of Conferences, **392**, 02041 (2023)
11. T.C. Carlson, D.A. Ripley, "On the relationship between NDVI, fractional vegetation," Remote Sens. Environ, 241–252 (1997)
12. J.A. Sobrino, J.C. Jimenez-Munoz, L. Paolini, "Land suface temperature retrieval from LANDSAT TM5," Remote Sensing of Environment, **90**, **4**, 434-440 (2004)
13. Landsat.usgs.gov, http://landsat.usgs.gov/landsat8.php
14. Statistical Yearbook of Thanh Hoa province for the years 2015 to 2020, Statistical Publishing House (2020)
15. Van, T.T.; Bao H.D.X.; Dinh Thi Kim Phuong Đ.T.K.; Mai N.T.T; Nhung Đ.T.M., "Characteristics of the thermal environment and urban heat island developments in the northern area of Ho Chi Minh City.," Journal of Can Tho University Science, **49**(A), 11-20 (2017)
16. Weatherspark, https://en.weatherspark.com/